International Geology Review, Vol. 48, 2006, p. 329–348.

Geology and Geochemistry of the Rapu-Rapu Ophiolite Complex, Eastern Philippines: Possible Fragment of the Proto–Philippine Sea Plate

G. P. YUMUL, JR.,[1]

Tectonics and Geodynamics Group, National Institute of Geological Sciences, College of Science, University of the Philippines, Diliman, Quezon City, Philippines and Philippine Council for Industry and Energy Research and Development, Department of Science and Technology, Bicutan, Taguig, Metro Manila, Philippines

C. B. DIMALANTA, R. A. TAMAYO, JR.,

Tectonics and Geodynamics Group, National Institute of Geological Sciences, College of Science, University of the Philippines, Diliman, Quezon City, Philippines

AND M. F. ZHOU

Department of Earth Sciences, University of Hong Kong, Pokfulam Road, Hong Kong, China

Abstract

The Cretaceous Rapu-Rapu Ophiolite Complex is a dismembered marginal basin ophiolite formed at an intermediate to fast spreading center. Limited subduction is manifested by the crystallization of pyroxene before plagioclase in the layered ultramafic cumulates. However, mafic cumulate rocks which exhibit the crystallization of plagioclase before pyroxene, consistent with low-water pressure conditions, could have formed in a mid-ocean ridge-like setting. Bulk-rock and trace-element analyses of volcanic-hypabyssal and gabbroic rocks show the predominance of a marginal basin geochemical signature. Spinel X_{Cr} ([Cr/Cr+Al] <0.60) suggests that the Rapu-Rapu peridotite and pyroxenite have mid-ocean ridge affinities. Fractional crystallization, and mantle-melt interaction together with melt replenishment, characterize the evolution of the ultramafic-mafic cumulate sequence; cryptic variation analysis reveals that the magma chamber operated as an open system. The Rapu-Rapu Ophiolite Complex, together with other fragments of the oceanic lithosphere exposed along the eastern Philippines, was probably derived from the proto–Philippine Sea plate.

Introduction

THE PHILIPPINE ISLAND ARC has attracted interest and studies because of its unique geological setting. It is bounded on the west by Sundaland and on the east by the Philippine Sea plate, and is made up of an agglomeration of terranes of varied origin (e.g., Yumul et al., 2001). Oppositely-dipping subduction zones serve as boundaries of this island arc system with that of the Sundaland and the Philippine Sea plate. Although there is general agreement that the Philippines formed to the south, the manner of transport to its present position is not yet well-constrained (e.g., Pubellier et al., 2003). Palinspastic reconstruction of Southeast Asia showed that during northwestward translation of the Philippines, it underwent clockwise rotation (Hall, 1996). Translation was made possible through slip along large-scale, bounding transcurrent faults. Workers have asserted that geologic study of the eastern Philippines can elucidate the origin and evolution of the ancient Philippine Sea plate (Deschamps et al., 2000; Hall, 2002).

The eastern Philippines is made up of regional metamorphic terranes (e.g., Geary et al., 1988; Billedo et al., 1996) and ophiolite complexes that are related to the proto-Philippine Sea plate (Tamayo et al., 2001). With this in mind, the geology and geochemistry of the Rapu-Rapu Ophiolite Complex of Rapu-Rapu Island, Bicol Province, southeastern Luzon were studied. Although the existence of an ophiolite complex on Rapu-Rapu Island was previously reported, no detailed description has yet been undertaken on it until now (David et al., 1996). We hope that the information presented here will

[1]Corresponding author; email: rwg@i-next.net or csrwg@yahoo.com

help in elucidating the early history of the Philippine Sea plate, in particular, and the reconstruction of the geological evolution of Southeast Asia, in general.

Regional Geology

The Philippine island arc system is located between two major converging plates—Sundaland in the west and the Philippine Sea plate on the east. A composite terrane consisting of blocks with varied affinities, it is characterized by subduction systems on both sides, and a major strike-slip fault zone that longitudinally traverses the island arc from north to south (Fig. 1). The downgoing plates that sandwich the arc include the east-dipping subduction zone along the Manila-Negros-Sulu-Cotabato trenches on the west, and the west-dipping subduction zone of the East Luzon Trough–Philippine Trench to the east. The Philippine fault zone, a left-lateral strike-slip fault, accommodates excess strain that cannot be absorbed by the surrounding trench systems. A large portion of the island arc belongs to the Philippine mobile belt, whereas the western side, which includes Mindoro, Palawan, the Sulu Sea, and the Zamboanga-Sulu Peninsula, is mapped as part of the Palawan microcontinental block (Faure et al., 1989; Yumul et al., 2004). A conspicuous feature of the Philippine island arc is the belt of ophiolitic complexes and metamorphic rocks that dot the eastern Philippines from Mati-Pujada, eastern Mindanao on the south through the Bicol Peninsula all the way to the Sierra Madre Range in eastern Luzon on the north (Fig. 1). Oceanic lithosphere has been recognized and mapped in Casiguran, Isabela-Baler, Caramoan Peninsula, Rapu-Rapu, Camarines Norte–Lagonoy, Giporlos, Dinagat and Mati-Pujada (e.g., Tamayo et al., 1996; Yumul et al., 1997).

Southeastern Luzon (Bicol Province), where the island of Rapu-Rapu is located, consists of the Bicol Peninsula and the Cagraray group of islands. The islands, aside from Rapu-Rapu, consist of Catanduanes, Cagraray, and Batan (Fig. 2). David et al. (1997) divided southeastern Luzon into three major structural units, north-central Catanduanes, and median and western Caramoan. These units are separated by two NW-SE–trending faults, the Hilawan and the Minas, respectively (Fig. 2). Rapu-Rapu Island, along with Cagraray and Batan, is part of the western Caramoan structural unit. This unit consists of a pre–Late Cretaceous ophiolite basement unconformably overlain by an Upper Cretaceous volcanic arc sequence. The latter, in turn, is unconformably overlain by a sequence of Middle Eocene limestone and Upper Oligocene–Pliocene carbonate and detrital strata. The section is capped by Pliocene–Quaternary volcanic and associated volcaniclastic rocks (David et al., 1997).

Geology of Rapu-Rapu Island

Our regional mapping of Rapu-Rapu Island revealed the presence of two terranes, Malobago and Pitogo, which are separated by a NNE-SSW–trending thrust fault with a possible strike-slip component (Fig. 2). The eastern, or Malobago block, consists of an intensely deformed metamorphic sequence, whereas the western, or Pitogo block, is underlain by a complete ophiolite suite (the Rapu-Rapu ophiolite complex). Excellent exposures crop out along the coasts of Malobago and Pitogo, after which we named the two blocks (Fig. 3).

Malobago block

The Malobago block comprises two-thirds of Rapu-Rapu Island in area. Intensely deformed and regionally metamorphosed rocks consisting of chlorite quartz schist, quartzofeldspathic mica schist, and quartz sericite schist were mapped (Fig. 4). Whole-rock ^{40}K-^{40}Ar dating on schist from the Malobago block yielded an Eocene age (42 ± 2 Ma) (Wolfe, 1981). Chlorite quartz schist is the most dominant of the three metamorphic rock types. This is usually greenish grey to greenish black and is composed of quartz, feldspar, and chlorite with varying amounts of epidote. This unit was probably derived from basic volcanic materials. Quartzofeldspathic mica schist is intercalated with the chlorite quartz schist. In some places, the quartzofeldspathic mica schist varies to quartzofeldspathic schist. This rock is light colored with epidote occurring only in small quantities; the probable protolith is dacitic volcanic rocks. Based on stratigraphic position, quartz sericite schist appears to occupy the uppermost section of the metamorphic rock complex. This rock is readily distinguished from the other units by its white color and softness. Furthermore, the quartz-sericite schist hosts the volcanogenic massive sulfide deposits found in the island.

The large and complicated folds observed in the metamorphic rocks attest to intense multiphase deformational events, which affected the island. Post-metamorphic deformation is suggested by localized structures like kink bands, chevron and

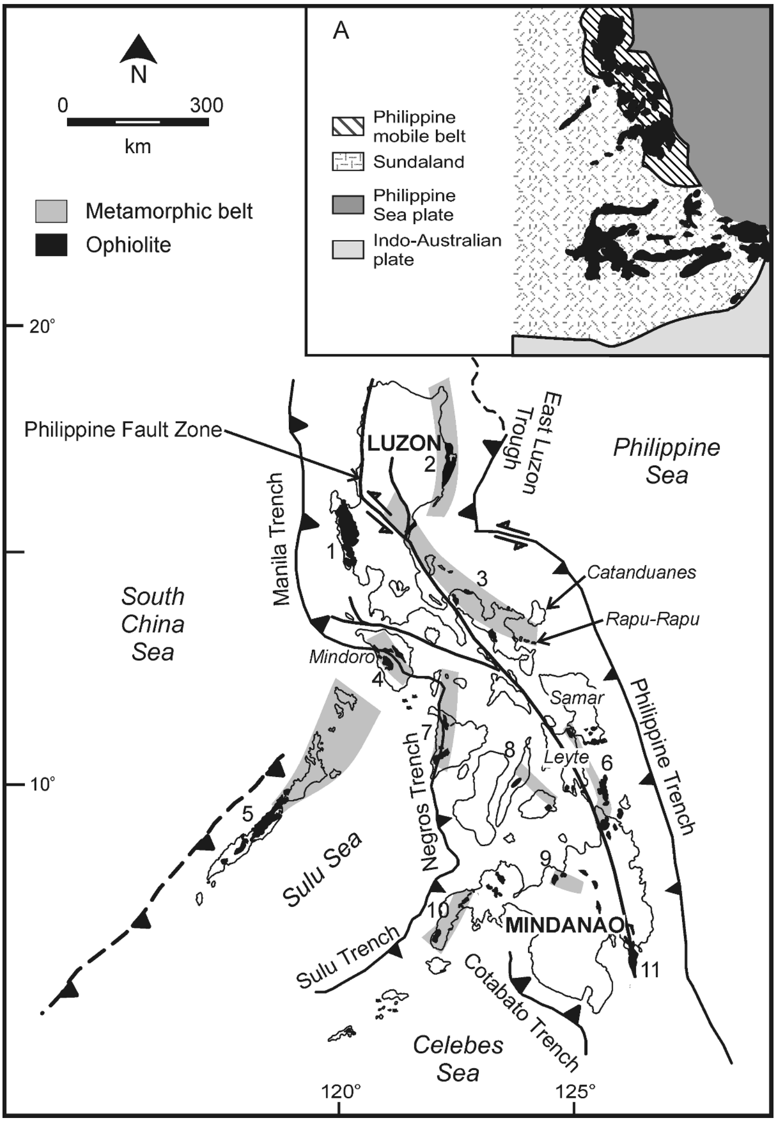

FIG. 1. Generalized tectonic map showing subduction systems surrounding the Philippines and major strike-slip fault zone traversing the island. It also shows the different metamorphic belts and ophiolite/ophiolitic complexes (modified from Bureau of Mines and Geosciences, 1982): 1 = Zambales; 2 = Casiguran (northern Sierra Madre); 3 = Isabela-Baler-Camarines Norte-Lagonoy-Rapu-Rapu (southern Sierra Madre–Bicol Peninsula); 4 = Mindoro; 5 = Palawan; 6 = Tacloban (Leyte)–Giporlos (Samar)–Dinagat; 7 = Antique; 8 = Cebu-Bohol; 9 = Central Mindanao; 10 = Zamboanga-Sulu Peninsula; 11 = Mati-Pujada. Inset A shows the Sundaland, Philippine Sea plate, and the Philippine mobile belt.

conjugate folds (Sherlock et al. 2003). The intercalation of chlorite quartz schist and quartzofeldspathic mica schist suggests different protoliths, volcaniclastic rocks derived from the erosion of basaltic and silicic rocks. These igneous rocks could have come from different volcanic centers or could be bimodal volcanism products from a single volcanic center. A dacitic protolith for the quartz sericite schist, which hosts the volcanogenic massive sulfides, is consistent with what has been

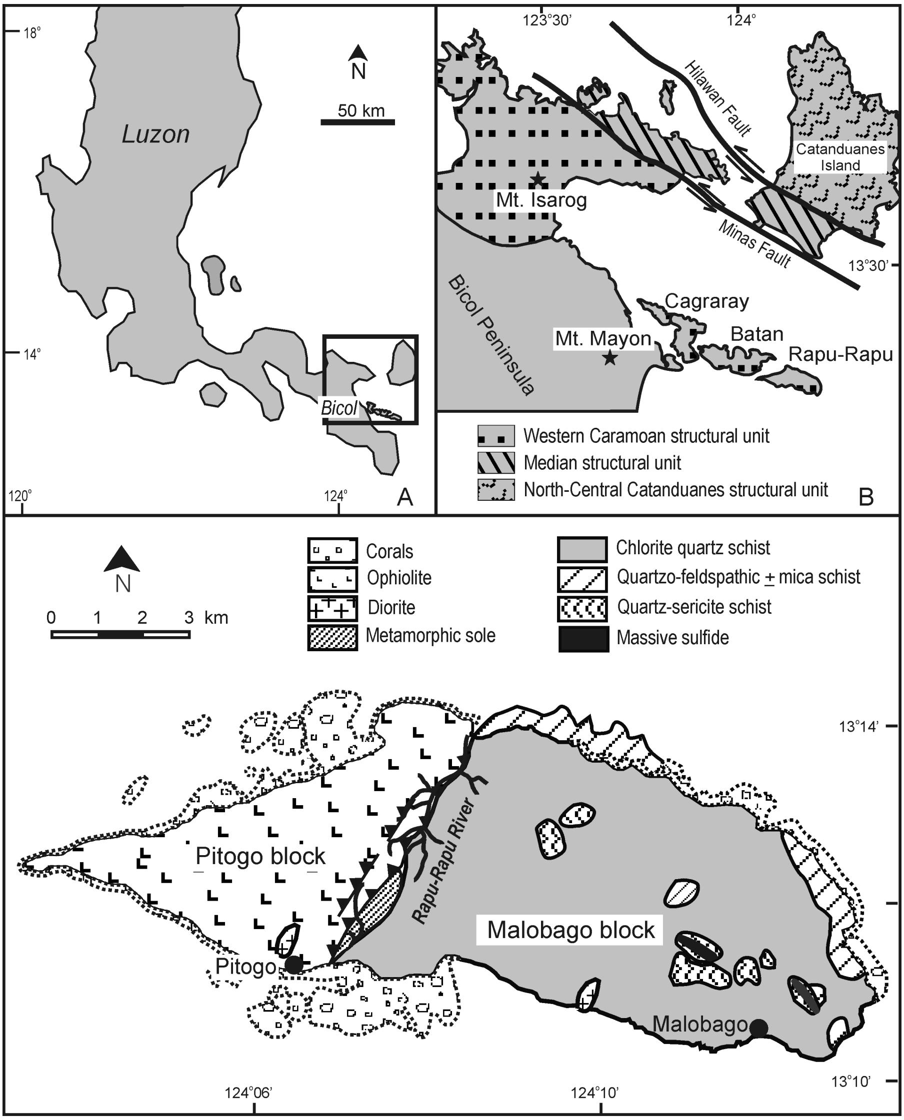

FIG. 2. Geologic map of the Rapu-Rapu Island, which is divided into two blocks—Pitogo and Malobago. The boundary between these two blocks is a NNE-SSW–trending thrust fault with a possible strike-slip component. Inset A is an index map showing the location of Bicol (boxed area). Inset B is the enlarged view of the boxed area in Inset A showing southeastern Luzon divided into three major structural units (north-central Catanduanes, western Caramoan, and Median). These units are bounded by two NW-SE trending faults, the Hilawan fault and the Minas fault (modified from David et al., 1997).

reported elsewhere (Barrett and MacLean, 1999; Querubin and Yumul, 2001).

Pitogo block

A complete ophiolite sequence composed of a harzburgite-dunite suite, layered pyroxenite, high-level and layered gabbro, dike swarm, and pillow basalt with manganiferous chert carapace was mapped in the Pitogo block. A thin amphibolite sliver is juxtaposed with the harzburgite and gabbro along the boundary between the Malobago and Pitogo blocks. The different members of the ophio-

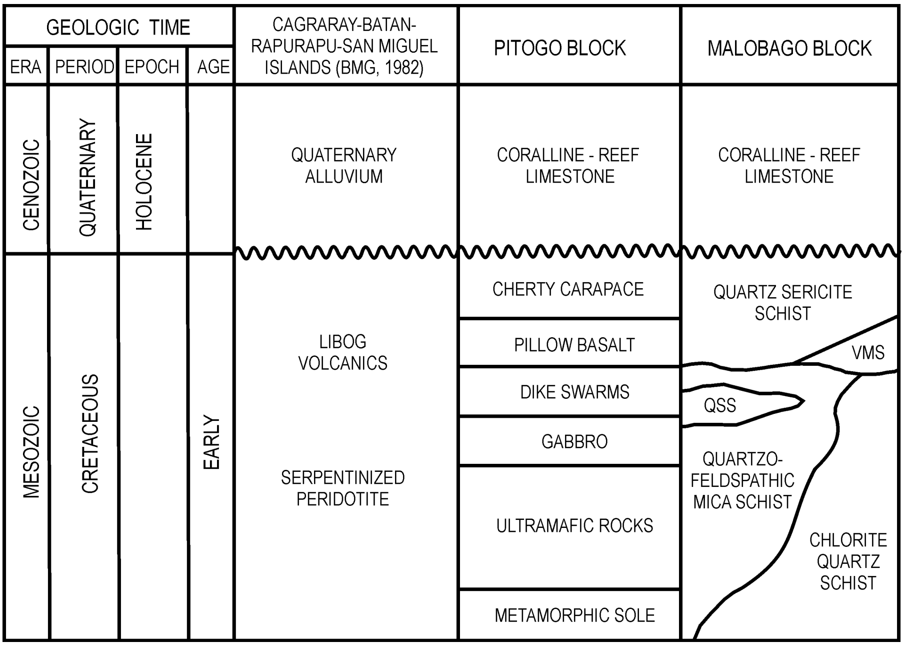

FIG. 3. Stratigraphic columns for the Pitogo and Malobago blocks compared with the stratigraphy proposed by the Bureau of Mines and Geosciences (1982) for the Cagraray–Batan–Rapu–Rapu–San Miguel islands. The eastern Malobago block consists of a metamorphic sequence, whereas the western Pitogo block is underlain by a complete ophiolite suite. Legend: QSS = quartz-sericite schist; VMS = volcanogenic massive sulfides.

lite complex are mostly exposed along the southern coast and the Rapu-Rapu River. Whole-rock ^{40}K-^{40}Ar dating of the diorite intruded into the harzburgite yielded a Late Cretaceous age of 77.1 ± 4.6 Ma (David et al., 1996), which defines the minimum age of this oceanic ultramafic-mafic sequence.

Generally, serpentinized harzburgite dominates the exposure of the Rapu-Rapu ophiolite complex. Sampling was concentrated along the coast because of the easy accessibility to this part of the island. Bastite is easily distinguished especially in harzburgite exhibiting hob-nail texture. Fresh harzburgite contains olivine, orthopyroxene, spinel, and in some cases, plagioclase. Clinopyroxene exsolution lamellae are present in orthopyroxene. Magnesite veinlets cut the orthopyroxene. Olivine is altered in varying degrees to serpentine and magnetite. Chromian spinel shows vermicular to holly-leaf textures. Amoeboid, pull-apart to subhedral and euhedral shapes of spinel also occur. Plagioclase is altered to either clay or carbonates. Some clinopyroxene porphyroclasts show bent lamellae. Harzburgite exhibits textures that range from protogranular to porphyroclastic. Dunite, exhibiting equigranular texture, is serpentinized. Olivine is altered to serpentine and magnesite. Brucite and talc veinlets transect the samples. Fresh vermicular clinopyroxene is also present locally. Chromian spinel is euhedral to subhedral.

A layered ultramafic cumulate sequence was mapped along the coast near Pitogo. The rocks consist of wehrlite, olivine websterite, and harzburgite. The layered sequence trends N30°W, with dips ranging from 68 to 85°NE. The wehrlite contains fresh olivine, orthopyroxene, clinopyroxene, and spinel. Vermicular plagioclase is altered to clay. The spinel is euhedral and fine grained compared to that found in the other layered ultramafic cumulate rocks. Some of the clinopyroxene is altered to metamorphic hornblende. Wehrlite, which has a mesocumulate texture, is tectonized with an apparent alignment of plagioclase and spinel. Olivine websterite, exhibiting mesocumulate texture, contains vermicular plagioclase, which is altered to clay. Chromian spinel present is euhedral to subhedral in shape. The orthopyroxene shows bent lamellae and

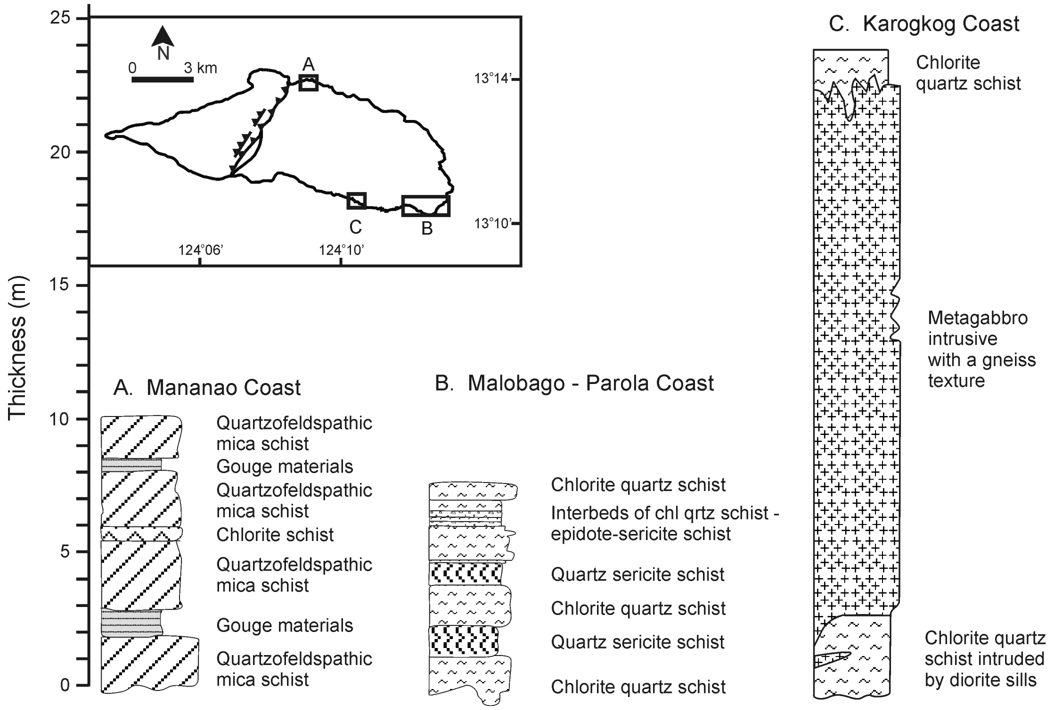

FIG. 4. Schematic diagram of section logs from the Malobago block, which is composed of intensely deformed metamorphic rocks. Logs shown correspond to the Mananao Coast, Malobago–Parola Coast, and Karogkog Coast. Inset shows the areas (box) from which the logs were taken. See text for discussion.

anomalous extinction. Clinopyroxene inclusions are present in orthopyroxene. Cumulate harzburgite within the layered cumulate sequence is made up of olivine and orthopyroxene with altered intercumulus plagioclase. Chromian spinel is euhedral to subhedral. The texture ranges from mesocumulate to adcumulate. Compared to the harzburgite, which is regarded as of residual origin, the cumulate harzburgite contains less clinopyroxene. The crystallization order for the layered ultramafic cumulate sequence is olivine ± spinel → clinopyroxene → orthopyroxene → plagioclase.

Layered gabbro float was encountered. *In situ* outcrops consist only of high-level gabbro, which is altered to varying degrees. Plagioclase is converted to clay and chlorite. Clinopyroxene is altered to either uralite or metamorphic hornblende. Quartz veinlets are common. Anomalous extinction is observed in clinopyroxene. Most of the crystals are anhedral and the dominant texture is orthocumulate. Based on the size and shape of minerals, the crystallization order is plagioclase → clinopyroxene.

The dike swarm contains andesite and diorite as exposed along the beach at Pitogo. The general trend is N70°W, dipping 55°SW. Pillow basalt contains microphenocrysts of acicular-shaped plagioclase set in fine-grained clinopyroxene. The basaltic pillow and dike swarm have undergone low-grade greenschist-facies metamorphism, which could be related to ocean-floor metamorphism. In Rapu-Rapu River, a thin sliver of amphibolite is in thrust contact with the harzburgite, gabbro, and underlying chlorite quartz schist. Whether this amphibolite corresponds to the metamorphic sole of an ophiolite needs to be looked into in the future. If this is the case, displacement has occurred to juxtapose the amphibolite with some of the gabbro instead of total contact with the residual harzburgite.

Methodology and Results of Analyses

Fused discs and pressed pellets of the volcanic-hypabyssal-gabbroic rocks were analyzed for major-

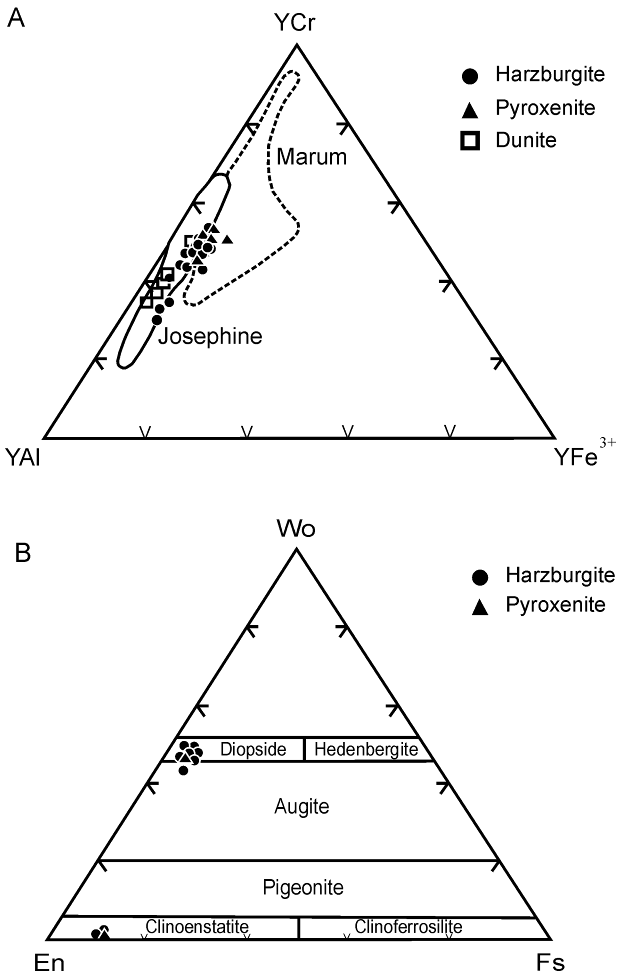

FIG. 5. A. YAl, YCr, and YFe^{3+} spinel diagram. The Rapu-Rapu Ophiolite Complex ultramafic rocks have spinel plotting between the Cr-Al tie line. The spinel analysed overlap the spinel compositional range of the Josephine (Dick, 1977) and Marum Complexes (Jaques, 1981). B. Wo-En-Fs diagram. Clinopyroxene in the ultramafic rocks is mostly diopside. Orthopyroxene plots in the clinoenstatite field.

and trace-element analysis using the Philips PW 1480 XRF of the Geological Institute, University of Tokyo. Details of the methodology, precision, and accuracy are presented in Yoshida and Takahashi (1997). Rare-earth elements were analyzed using a VG Element PlasmaQuad 3 ICP-MS at the Department of Earth Sciences, University of Hong Kong utilizing a procedure described in Jenner et al. (1990). An international standard, the Hawaiian basalt BHVO, analyzed to monitor the accuracy and precision of the instrument, showed that the results are within the 1σ error range of recommended values. Mineral chemistry analysis was done using the JEOL JCMA 733 mkII microprobe of the Geological Institute, University of Tokyo with correction following that of Nakamura and Kushiro (1970). Details of the procedure are presented elsewhere (Yumul, 1989).

Olivine from residual harzburgite and ultramafic cumulate rock displays similar and relatively

TABLE 1. Representative Mineral Chemistry of Rapu-Rapu Olivine from Residual Harzburgite and Ultramafic Cumulate Rocks[1]

	RAP-15 Hz	RAP 102 Hz	RAP 106 Hz	RAP 104 Hz	RAP 110 Hz	RAP 100 Hz	RAP 101 Hz	RAP 108 Hz	RAP 3 Hz	RAP 60 Hz	RAP - 59 Hz	RAP-56 We	RAP 58 Ol Wb
SiO_2	40.45	39.57	40.74	37.95	41.50	40.91	40.63	40.52	40.12	40.18	39.83	39.73	40.51
TiO_2	0.00	0.01	0.00	0.03	0.00	0.05	0.00	0.00	0.01	0.00	0.03	0.00	0.01
Al_2O_3	0.00	0.00	0.00	0.02	0.00	0.02	0.00	0.01	0.00	0.00	0.01	0.01	0.01
V_2O_3	0.03	0.00	0.00	0.03	0.00	0.01	0.03	0.00	0.01	0.04	0.00	0.00	0.00
FeO	9.01	9.84	9.80	9.91	9.09	9.76	9.62	9.35	10.01	10.16	10.19	10.56	9.36
MnO	0.12	0.13	0.17	0.13	0.15	0.11	0.09	0.22	0.13	0.17	0.15	0.12	0.21
MgO	49.27	49.83	49.54	50.42	49.81	50.04	49.53	50.85	49.28	49.42	48.89	49.12	49.81
CaO	0.00	0.04	0.01	0.04	0.05	0.01	0.03	0.01	0.02	0.02	0.02	0.02	0.03
Cr_2O_3	0.00	0.05	0.00	0.07	0.02	0.05	0.00	0.00	0.02	0.01	0.04	0.00	0.05
NiO	0.45	0.40	0.41	0.40	0.40	0.42	0.45	0.46	0.42	0.41	0.30	0.38	0.45
Total	99.33	99.87	100.67	99.00	101.02	101.38	100.38	101.42	100.02	100.41	99.46	99.94	100.44
						Cations (oxy = 4)							
Ol Fo	0.907	0.900	0.900	0.901	0.907	0.901	0.902	0.906	0.898	0.897	0.895	0.892	0.905

[1]Hz, = harzburgite; We = wehrlite; Ol Wb = olivine websterite.

TABLE 2. Representative Mineral Chemistry of Rapu-Rapu Spinel from Residual Dunite and Layered Ultramafic Rocks[1]

	RAP-12	RAP-13	RAP-15	RAP 102	RAP 106	RAP 104	RAP 110	RAP 100	RAP 101	RAP 3	RAP 60	RAP - 59	RAP-56	RAP 58
	Dun	Dun	Hz	Hz	Hz	Hz	Hz	Hz	Hz	Hz	Hz	Hz	We	Ol Wb
	SPC2	SPC2	SPC2	SP C1	SP C2	SP C1	SP C1	SP C1	SP C1	SP C2	SP C1	SP C2	SPC2	SP C1
SiO_2	0.46	0.03	0.06	0.05	0.02	0.05	0.02	0.44	0.04	0.01	0.03	0.01	0.00	0.02
TiO_2	0.12	0.04	0.08	0.00	0.06	0.07	0.04	0.03	0.05	0.27	0.39	0.56	0.50	0.31
Al_2O_3	31.66	32.75	24.40	56.25	55.83	54.90	32.30	62.24	56.02	35.08	24.61	23.42	22.29	22.18
V_2O_3	0.22	0.21	0.34	0.06	0.12	0.07	0.24	0.04	0.04	0.23	0.28	0.41	0.42	0.25
Cr_2O_3	34.40	33.66	37.87	12.60	12.25	13.00	34.01	5.65	12.92	28.53	37.56	38.29	39.76	42.20
FeO	18.06	18.56	24.21	12.09	12.06	12.52	19.07	10.06	12.20	21.88	24.12	26.00	25.63	24.13
MnO	0.25	0.21	0.26	0.09	0.11	0.12	0.17	0.08	0.08	0.21	0.26	0.28	0.30	0.35
MgO	14.63	13.78	10.47	19.24	18.83	19.04	14.08	21.18	19.16	13.13	10.95	10.39	10.15	10.28
CaO	0.02	0.01	0.01	0.02	0.01	0.03	0.02	0.00	0.00	0.02	0.05	0.03	0.03	0.03
NiO	0.14	0.12	0.11	0.33	0.35	0.28	0.19	0.63	0.37	0.17	0.14	0.16	0.16	0.14
Total	99.95	99.35	97.81	100.73	99.62	100.07	100.13	100.34	100.87	99.52	98.38	99.55	99.23	99.89
							Cations (oxy = 4)							
XCr	0.422	0.408	0.510	0.131	0.128	0.137	0.414	0.057	0.134	0.353	0.506	0.523	0.545	0.561
XMg	0.634	0.609	0.495	0.751	0.744	0.750	0.619	0.799	0.747	0.575	0.511	0.482	0.476	0.482
YCr	0.406	0.394	0.475	0.130	0.128	0.135	0.395	0.057	0.133	0.333	0.470	0.481	0.503	0.528
YAl	0.557	0.571	0.456	0.863	0.867	0.852	0.560	0.937	0.860	0.610	0.459	0.438	0.420	0.413
YFe^{3+}	0.038	0.035	0.068	0.008	0.005	0.013	0.045	0.006	0.007	0.056	0.072	0.081	0.077	0.059

[1]Dun = dunite; Hz = harzburgite; We = wehrlite; Ol Wb = olivine websterite.

TABLE 3. Representative Mineral Chemistry of Rapu-Rapu Clinopyroxene and Orthopyroxene from Residual and Cumulate Ultramafic Rocks[1]

	RAP 13	RAP 15		RAP 102		RAP 106		RAP 104		RAP 110		RAP 100		RAP 101		RAP 7	RAP 3		RAP 60	RAP 59		RAP 56	RAP 58	
	Dun	Hz		Hz		Hz		Hz		Hz		Hz		Hz		Hz	Hz		Hz	Hz		We	Ol Wb	
	Cpx	Cpx	Opx	Opx	Cpx	Opx	Cpx	Opx	Cpx	Opx	Cpx	Opx	Cpx	Opx	Cpx	Cpx	Opx	Cpx	Opx	Opx	Cpx	Opx	Opx	Cpx
SiO_2	53.68	52.64	55.15	54.85	53.21	54.72	52.82	55.02	52.04	56.15	53.57	55.38	52.98	55.66	52.87	51.96	54.74	51.37	55.70	55.81	52.62	55.30	56.23	53.31
TiO_2	0.06	0.13	0.05	0.11	0.31	0.08	0.31	0.04	0.37	0.02	0.09	0.03	0.22	0.07	0.27	0.57	0.17	0.57	0.13	0.14	0.42	0.18	0.10	0.20
Al_2O_3	1.98	3.53	3.14	4.70	4.64	4.00	5.11	3.78	6.40	3.08	3.86	5.63	6.02	4.36	5.66	6.14	3.27	4.15	1.75	1.78	2.78	1.91	1.92	2.65
Fe_2O_3																								
FeO	2.11	2.37	6.04	6.04	2.92	6.39	2.41	6.28	2.30	6.03	2.35	6.61	3.01	6.39	2.73	2.49	6.71	2.91	6.73	6.96	2.76	6.67	6.42	2.56
MnO	0.06	0.11	0.17	0.18	0.07	0.15	0.02	0.11	0.09	0.12	0.07	0.13	0.07	0.12	0.11	0.09	0.13	0.09	0.15	0.16	0.09	0.15	0.17	0.05
MgO	17.52	16.74	33.88	32.52	17.15	33.05	15.82	33.64	15.35	33.82	17.03	32.67	16.84	33.19	16.40	15.04	32.88	15.88	33.80	33.40	16.51	33.33	33.98	17.43
CaO	23.91	23.43	0.89	1.14	21.11	0.79	22.79	0.74	23.19	1.42	23.63	1.00	21.19	0.78	21.87	21.56	0.94	22.91	0.76	0.86	23.27	1.15	0.90	23.14
Na_2O	0.21	0.35	0.00	0.06	0.66	0.02	0.65	0.02	0.78	0.00	0.28	0.03	0.79	0.06	0.81	1.43	0.01	0.48	0.02	0.01	0.37	0.01	0.04	0.36
Cr_2O_3	0.70	0.94	0.62	0.54	0.66	0.37	0.80	0.41	1.15	0.57	0.97	0.37	0.46	0.41	0.90	0.67	0.72	1.11	0.39	0.42	0.85	0.58	0.50	0.96
Total	100.22	100.23	99.94	100.14	100.72	99.57	100.74	100.06	101.67	101.21	101.83	101.85	101.57	101.03	101.61	99.96	99.57	99.47	99.43	99.54	99.67	99.26	100.25	100.65
												cations (oxy = 6)												
Wo	47.8	48.2	1.7	2.22	44.62	1.53	48.80	1.42	49.96	2.66	48.02	1.94	45.06	1.49	46.64	48.45	1.81	48.39	1.44	1.63	48.00	2.17	1.70	46.81
En	48.8	47.9	89.1	88.30	50.44	88.63	47.12	89.09	46.02	88.32	48.16	87.88	49.83	88.74	48.65	47.03	87.93	46.65	88.46	87.86	47.40	87.76	88.66	49.07
Fs	3.4	4.0	9.2	9.48	4.94	9.85	4.07	9.50	4.02	9.02	3.83	10.18	5.11	9.77	4.72	4.52	10.27	4.96	10.10	10.52	4.60	10.07	9.65	4.11
XMg	95.8	95.4	93.4	90.88	91.29	91.75	92.11	92.74	93.82	92.42	93.37	90.02	91.86	90.69	92.58	94.83	91.24	93.46	92.00	90.82	92.89	91.93	92.02	95.46

[1]Hz = harzburgite; we = wehrlite; ol wb = olivine websterite.

TABLE 4. Representative Whole-Rock and Trace-Element Compositions of Gabbro, Diorite, and Basalt from Rapu-Rapu[1]

	RAP-1 Gab	RAP-2 Gab	RAP-8 Gab	RAP-62 Gab	RAP-63 Gab	RAP-64 Gab	RAP-52 Dio	RAP-53 Dio	RAP-54 Bst	RAP-55 Bst
					wt%					
SiO_2	48.15	47.96	47.41	46.85	48.02	50.59	53.44	54.99	49.58	49.55
TiO_2	0.41	0.45	0.43	1.02	1.71	1.29	0.70	0.55	0.97	1.00
Al_2O_3	19.39	18.67	17.85	17.03	14.91	14.97	18.23	18.24	17.58	17.37
Fe_2O_3	6.73	7.41	6.86	9.93	11.69	10.18	7.17	6.31	8.11	8.17
MnO	0.11	0.12	0.13	0.19	0.19	0.18	0.13	0.10	0.14	0.14
MgO	9.28	10.20	10.23	8.84	7.71	7.78	7.24	6.77	9.52	9.39
CaO	12.38	12.60	15.22	12.45	10.65	10.69	7.63	7.97	10.09	10.44
Na_2O	2.81	2.49	1.38	2.59	3.89	3.98	4.79	3.98	3.30	3.26
K_2O	0.04	0.02	0.04	0.11	0.02	0.05	0.38	0.36	0.20	0.16
P_2O_5	0.04	0.03	0.06	0.10	0.14	0.13	0.10	0.08	0.09	0.10
Total	99.35	99.94	99.61	99.13	98.94	99.85	99.82	99.35	99.59	99.60
					ppm					
Sc	26	29	34	36	45	35	28	24	26	27
V	115	134	160	241	375	284	162	142	154	163
Cr	803	895	1097	497	297	403	298	253	412	399
Ni	176	185	202	127	65	88	94	104	184	178
Rb	0.7	0.5	0.7	1.4	0.3	0.9	1.8	1.6	0.8	0.8
Sr	122	126	159	143	132	106	274	267	167	154
Y	10	10	9	21	31	26	12	10	17	19
Zr	15	15	16	48	97	78	61	46	62	64
Nb	0.3	0.2	0.2	0.7	0.9	1.0	1.4	1.1	0.7	0.6
Ba	49	46	52	47	44	45	68	58	53	47
La	0.5	0.7	0.5	1.4	2.2	2.1	2.3	2.0	1.2	1.3
Ce	1.6	1.7	1.8	5.1	7.9	7.5	6.6	5.5	5.1	5.4
Pr	0.3	0.4	0.3	1.0	1.5	1.4	1.1	0.9	1.1	1.2
Nd	2.1	2.4	2.1	5.9	8.5	8.1	5.6	4.6	6.8	7.0
Sm	0.9	1.0	0.9	2.3	3.2	3.0	1.7	1.4	2.4	2.5
Eu	0.5	0.6	0.5	0.9	1.1	1.1	0.6	0.5	0.9	0.9
Gd	1.3	1.5	1.4	3.1	4.5	3.9	2.0	1.6	3.0	3.2
Tb	0.2	0.3	0.3	0.6	0.8	0.7	0.4	0.3	0.5	0.5
Dy	1.7	1.9	1.7	3.8	5.6	4.7	2.3	1.8	3.4	3.6
Ho	0.4	0.4	0.4	0.8	1.2	1.0	0.5	0.4	0.7	0.8
Er	1.1	1.2	1.1	2.4	3.6	3.0	1.4	1.1	2.1	2.1
Tm	0.2	0.2	0.2	0.4	0.5	0.4	0.2	0.2	0.3	0.3
Yb	1.1	1.1	1.1	2.5	3.6	3.0	1.4	1.1	2.1	2.1
Lu	0.1	0.2	0.1	0.3	0.5	0.4	0.2	0.2	0.3	0.3
Hf	0.4	0.4	0.5	0.9	0.9	1.2	1.2	0.9	1.7	1.7
Ta	0.2	0.0	0.0	0.1	0.1	0.1	0.1	0.1	0.1	0.1
Pb	0.5	4.3	0.0	0.0	2.6	0.7	0.5	0.2	0.0	0.1
Th	0.0	0.2	0.0	0.0	0.0	0.1	0.1	0.1	0.0	0.0
U	0.0	0.1	0.0	0.0	0.0	0.1	0.0	0.1	0.0	0.0

[1]Gab = gabbro; Dio = diorite: Bst = basalt.

limited $Fo_{0.90–0.91}$ and $Fo_{0.894–0.905}$ ranges, respectively (Table 1). Spinel from residual dunite and harburgite shows relatively low X_{Cr} [Cr/(Cr+Al)] (0.42 to 0.48 and 0.065 to 0.39, respectively) compared to the layered ultramafic rocks (0.51–0.54). Residual dunite and layered ultramafic rock spinel exhibit limited $Y_{Cr0.4–0.46}$ $Y_{Al0.49–0.56}$ $Y_{Fe^{3+}0.03–0.05}$ (trivalent ion/ΣCr+Al+Fe^{3+}) and $Y_{Cr0.48–0.5}$ $Y_{Al0.43–0.45}$ $Y_{Fe^{3+}0.06-0.08}$ ranges compared to the residual harzburgite spinel range of $Y_{Cr0.06–0.45}$ $Y_{Al0.5–0.93}$ $Y_{Fe^{3+}0.01-0.06}$ (Fig. 5A; Table 2). Clinopyroxene from residual peridotite shows a wider X_{Mg} [Mg/(Mg+Fe^{2+})] range (0.91 to 0.97) than those from the layered ultramafic cumulate rock suite (0.93–0.95). The clinopyroxene from peridotite is mostly diopside; chromiferous diopside occurs less frequently in residual harzburgite (Fig. 5B; Table 3). Clinopyroxene in the high level gabbro is replaced by secondary amphibole. Orthopyroxene displays narrow X_{Mg} ranges for both residual and cumulate ultramafic rocks (0.91–0.93 and 0.91–0.92, respectively) (Fig. 5B; Table 3). Relict plagioclase in the peridotite was not analyzed because it was altered to clay.

The rocks show relatively low rare-earth element (REE) concentrations (Table 4). For example, the basalts are depleted in light (L)REE and heavy (H)REE compared to the N-MORB concentrations reported by Sun and McDonough (1989). $(La/Yb)_n$ and $(La/Sm)_n$ ratios are very low in both the basalts (0.38–0.40 and 0.3–0.32) and the gabbros (0.31–0.48 and 0.36–0.44), but are high in the diorites (1.12–1.17 and 0.87–0.91). Thorium and Nb concentrations in these rocks are very low as well and they increase from the gabbros (below detection to 0.24 ppm and 0.15 to 0.95 ppm, respectively) through the basalts (0.04 ppm and 0.58–0.65 ppm) to the diorites (0.05–0.08 ppm and 1.14–1.35 ppm).

The rare-earth element concentrations normalized to C1 chondrite values after Boynton (1984) of the rocks are given in Figure 6A. In both the basalts and gabbros, they display generally flat patterns from the HREE toward the middle (M)REE, coupled with decreasing patterns from the MREE toward the LREE. By contrast, the diorites show slightly increasing patterns from the HREE toward the LREE. Except for one gabbro, all the multi-element concentrations normalized to primitive mantle values of Sun and McDonough (1989) of the rocks exhibit decreasing patterns from the HREE to Th and Nb (Fig. 6B). The gabbro, on the other hand, shows weak and clear negative anomalies in Ti and Nb, respectively.

Discussion

Rapu-Rapu ophiolite complex: A marginal basin ophiolite

The Rapu-Rapu ophiolite complex, although dismembered, is a complete ophiolite sequence. Outcrops of residual harzburgite underlying layered ultramafic cumulate sequence that is, in turn, overlain by high level gabbro suggest the existence of a magma chamber. Layered gabbro float, representing fragments of magma chamber cumulate rocks, have also been described. A dike swarm complex and pillow lava suite complete the crust-mantle sequence. These units crop out in the Pitogo block.

Intercalations of pillow lavas and metamorphosed volcaniclastic sediments that might correspond to the sedimentary cover of the Rapu-Rapu ophiolite complex are present in the Malobago block. The composition of the volcaniclastic sediments suggests that the whole complex (ophiolite + metamorphic suite) could have formed adjacent to a landmass. Moreover, if the pillow lavas in the Malobago block are related to the volcanic rocks of the Rapu-Rapu ophiolite complex, then the metamorphosed sediments intercalated within the lavas may indicate gaps in volcanism. Harzburgite is not immediately overlain by pillow lavas; gabbro pods within the harzburgite, which is a notable feature in slow-spreading centers, are not present. These field observations are consistent with the idea of generation of the Rapu-Rapu crust-mantle sequence in an intermediate to fast-spreading center (Dilek et al., 1998; Yumul, 2003).

The crystallization order of the layered ultramafic cumulate sequence shows the appearance of clinopyroxene and orthopyroxene ahead of the plagioclase, similar to the order noted in subduction-related magmas (Beard, 1986; Bloomer et al., 1995). Recent works, nonetheless, have ascribed the formation of orthopyroxene through hydrothermal rather than magmatic processes. This is particularly true in the Oman ophiolite wherein the pyroxene is thought to be related to seawater-rock interaction in a mid-ocean ridge environment (Benoit et al., 1999; Koga et al., 2001).

The subduction influence, although present, was not dominant as the chemistry of spinel ($XCr < 0.60$) is similar to spinel found in mid-ocean ridge abyssal peridotite rather than those related to island arc rocks (Dick and Bullen, 1984; Barnes and Roeder, 2001; Kamenetsky et al., 2001; Coish and Gardner, 2004). The crystallization order among the high-

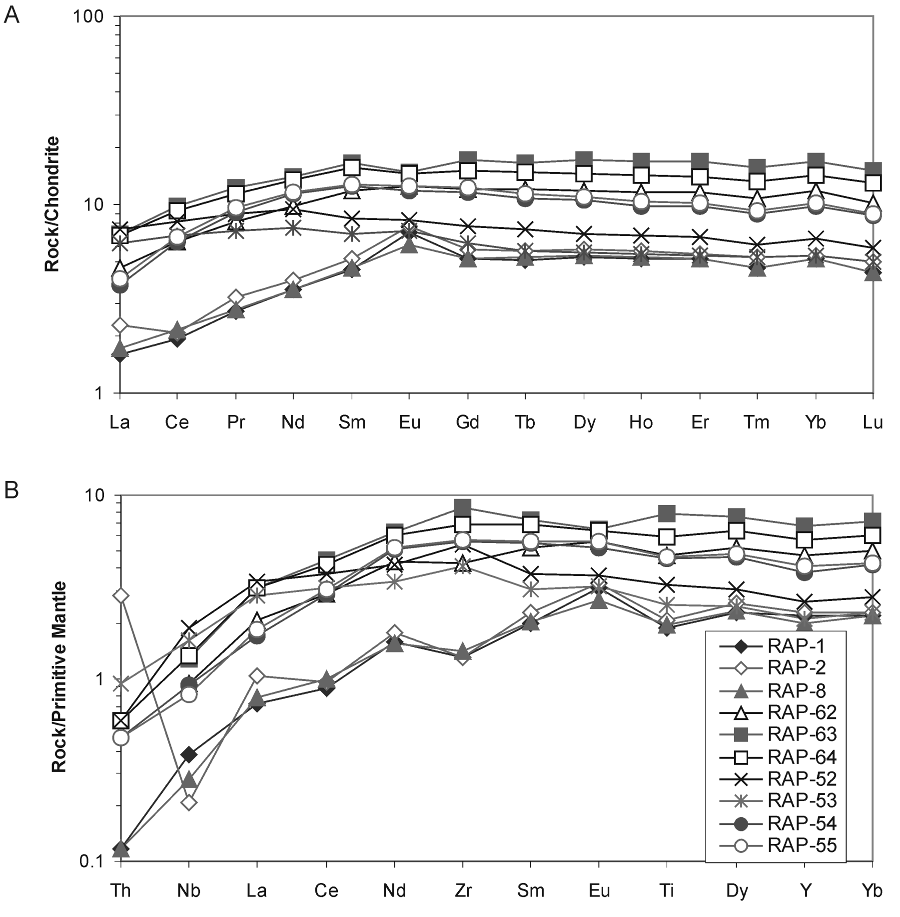

FIG. 6. A. Rare-earth element concentrations of the rocks normalized to the C1 chondrite values from Boynton (1984). See text for discussion. B. Except for one gabbro, all multi-element concentrations of the rocks normalized to primitive mantle values of Sun and McDonough (1989) exhibit decreasing patterns from the HREE to Th and Nb.

level gabbro is not consistent with subduction process, inasmuch as plagioclase fractionated prior to pyroxene, suggesting an occurrence at low-water fugacity typical of the mid-ocean ridge environment. This combination of island arc and mid-ocean ridge geochemical characteristics can be accounted for if the Rapu-Rapu ophiolite complex was formed in a marginal basin. Rocks collected from several modern marginal basins display muted island arc geochemical signatures, which are dominated by MOR geochemical affinities (Gribble et al., 1998; Falloon et al., 1999).

The present-day geographic location of the ophiolite complex would place it in a forearc setting with respect to the Philippine Trench (Fig. 2). Although most ancient lithospheric complexes are reported to have formed in a back-arc basin setting, this may not necessarily be applicable for the Rapu-Rapu ophiolite complex (e.g., Pfander et al., 2002; Wang et al., 2002). For one thing, locations of the trench and arc associated with the Rapu-Rapu body are difficult to constrain. However, the available field evidence, specifically the presence of volcaniclastic sediments intercalated and on top of the ophiolite, suggests that this oceanic lithosphere originated in a land-bounded ocean basin, similar to the configuration of modern marginal basins and other recognized back-arc basin ophiolites (e.g., Yumul, 1993).

It is clear that the chemical compositions, the REE, and multi-element patterns of the rocks are typical of MOR or marginal basin (e.g., Saunders and Tarney, 1984; Xu et al., 2003; Tamayo et al.,

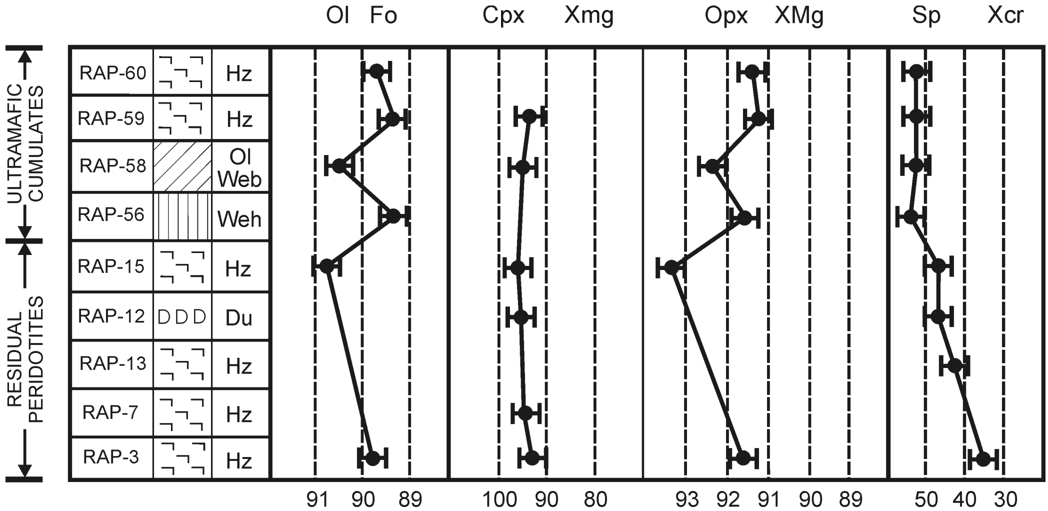

FIG. 7. Cryptic variation of the residual-cumulate sequence of the Rapu-Rapu ophiolite complex. RAP-3 to RAP-15 are residual rocks, whereas the rest are cumulate rocks. An increase in the olivine forsterite and orthopyroxene XMg as shown by RAP-58, suggests introduction of a primitive melt. However, clinopyroxene XMg and spinel XCr of RAP-58 are decoupled and do not show what the olivine and orthopyroxene data suggest.

2004) (Figs. 6A and 6B). Their very low trace-element concentration can be related either to mantle source partial melting degrees higher than those which modern magma sources in MOR settings undergo, or to multiple episodes of partial melting. Marginal basin rocks, particularly those affected by suprasubduction processes, characteristically show these chemistries (Pearce et al., 1984; Hawkins, 1995). Notable among the rocks from Rapu-Rapu island is a gabbro (RAP-2) that displays negative anomalies in Nb and Ti. This signature is typical of subduction-related lavas, such as those emplaced on arcs or back-arc basins (e.g., Shervais, 2001).

Partial melting, mantle-melt interaction, and crystallization processes: Constraints from the ultramafic rocks

The cryptic variation of minerals from a section representing residual harzburgite to layered ultramafic cumulate rocks shows evidence of varying degrees of partial melting, crystallization, and small inputs of more primitive magmas (Fig. 7). For the residual rocks, the clinopyoxene shows limited X_{Mg} values; the spinel X_{Cr} shows a general increase in the degree of partial melting from RAP-3 through RAP-13 all the way to RAP-15. This is consistent with the increase in the olivine Fo and orthopyroxene X_{Mg} from the lowermost residual harzburgite to RAP-15, which underlies the layered ultramafic cumulate sequence.

In the layered ultramafic cumulate sequence, clinopyroxene X_{Mg} and spinel X_{Cr} show a very slight decrease from the olivine websterite (RAP-58) to the stratigraphically higher layered harzburgite. These are trends normally exhibited by a fractionating magma chamber. In contrast, olivine Fo and orthopyroxene X_{Mg} display kinks between lithologic units in the layered sequence, from the wehrlite (RAP-56) to olivine websterite (RAP-58), and from harzburgite (RAP-59) to another harzburgite (RAP-60) (Fig. 7). Such a pattern suggests input of melt more primitive in composition than the fractionating magma in the chamber. However, even though it appears that replenishment of new magmas occurred, this was not a major evolutionary process, inasmuch as there is a decoupling in the chemistry of the four principal minerals, as seen in RAP-58.

The olivine X_{Mg} versus NiO (wt%) shows a limited increase in the degree of partial melting among harzburgite (Fig. 8A). Following Sato's (1977) calculations, a plot of the layered pyroxenite suggests that it has been affected by fractional crystallization (Fig. 8A). The plot of the rocks on the olivine Fo versus spinel X_{Cr} diagram show that at the same olivine Fo, the Rapu-Rapu harzburgite and pyroxenite have similar to higher spinel X_{Cr} values compared to

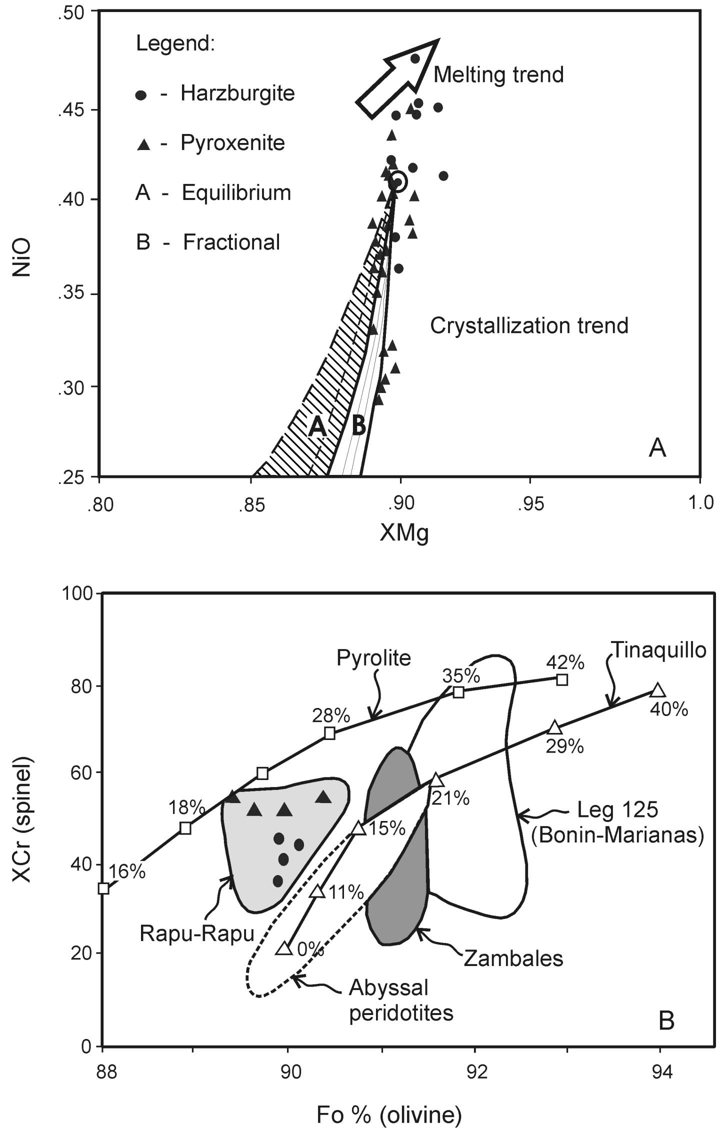

FIG. 8. A. The olivine Fo versus NiO shows that pyroxenites have undergone fractional crystallization. Crystallization trend after Sato (1977). B. The olivine Fo versus spinel XCr suggests that Rapu-Rapu samples have undergone less than 15% of partial melting based on the Tinaquillo tie line. Tinaquillo and pyrolite partial melting trends are after Jaques and Green (1980). Zambales field is after Yumul (1992); Leg 125 field after Parkinson and Pearce (1998).

abyssal peridotite. Furthermore, the Rapu-Rapu harzburgite and pyroxenite mantle source have also undergone lower degrees of partial melting (i.e., less than 15% partial melting, following the Tinaquillo peridotite partial melting trend) as compared to the Zambales ophiolite complex and the Leg 125 Bonin-Marianas site (Yumul, 1992; Parkinson and Pearce, 1998) (Fig. 8B). This relatively low degree of partial melting is consistent with the geochemical signatures exhibited by the basalt, gabbro, and diorite (Figs. 6A and 6B).

As previously mentioned, the spinel from the harzburgite, dunite, and pyroxenite shows $X_{Cr} < 0.60$ (Fig. 9A). Subsolidus re-equilibration could

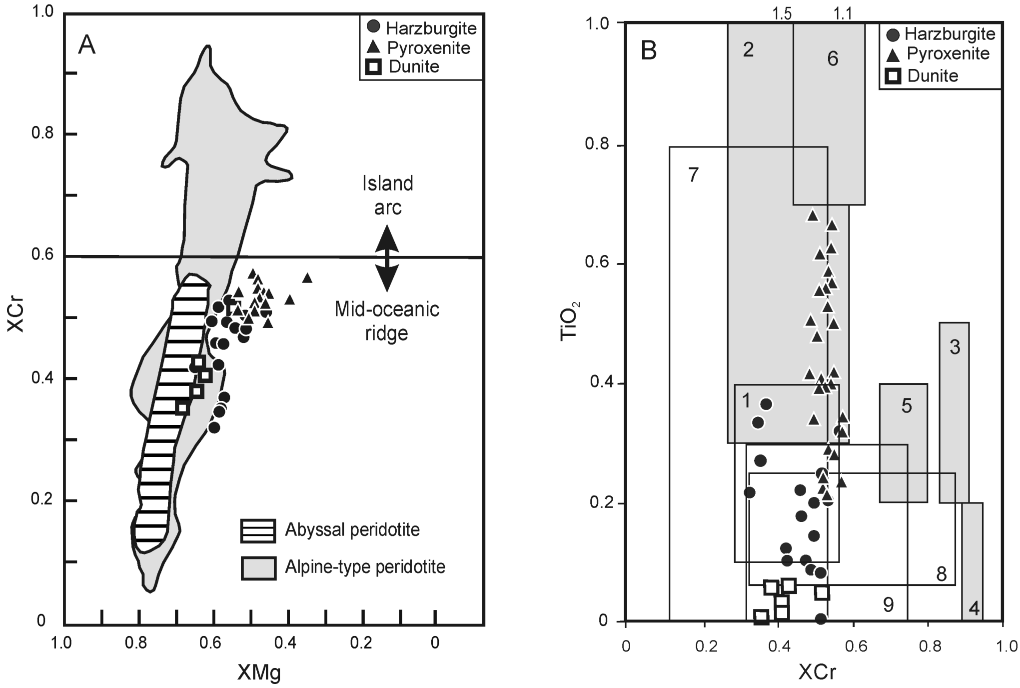

FIG. 9. A. Spinel from the different ultramafic rocks and spinel found among ultramafic rocks in mid-ocean ridge settings are almost similar. The shift to the right of the sample sets can be attributed to subsolidus re-equilibration with respect to XMg. Fields after Dick and Bullen (1984). B. The increase in spinel TiO_2 at a limited range of spinel XCr suggests mantle-melt interaction. Spinel XCr and TiO_2 fields taken from Kamenetsky et al. (2001): 1 = FAMOUS, Mid-Atlantic Ridge, MORB; 2 = Macquarie, Southwest Pacific, MORB; 3 = Vanuatu high-K and CA series; 4 = Papua New Guinea boninites; 5 = Troodos boninites; 6 = West Greenland, Large Igneous Province; 7 = mid-ocean ridge mantle peridotites; 8 = Izu-Mariana mantle peridotites; and 9 = New Caledonia mantle peridotites. See text for discussion.

have caused the spread in the spinel X_{Mg}. The range of spinel X_{Cr} shown by the rocks is similar to those exhibited by peridotite and pyroxenite formed in mid-ocean ridge environments rather than those of island-arc settings. Although this is the case, it is assumed that the water pressure was relatively high to enable the crystallization of pyroxene ahead of plagioclase among the layered ultramafic rocks, as well as the formation of orthopyroxene and crystallization of gabbro instead of troctolite in the mafic cumulate sequence. This setting would be similar to that of a marginal basin that is affected by limited subduction component.

In terms of the spinel X_{Cr} versus TiO_2 (wt%), the dunite spinel plots in the depleted portion (<0.1% TiO_2) of the mid-ocean ridge mantle peridotite field (e.g., Kamenetsky et al., 2001) consistent with its residual origin (Fig. 9B). The X_{Cr} in harzburgite positively correlates with TiO_2 (wt%). Again, this agrees with increasing degrees of partial melting. Moreover, the chemistry of the Rapu-Rapu ophiolite complex peridotite is within the composition range of the Nikanbetsu peridotite complex (0–0.6 spinel TiO_2) in Hokkaido, Japan and abyssal plagioclase-bearing peridotites (TiO_2 0.10–1.45 wt%; XCr 0.1 to 0.6) (Brunelli et al., 2003; Takahashi, 2001).

The dunite was not a residue left by the partial melting of the harzburgite with high X_{Cr} and low TiO_2 (wt%) because the dunite X_{Cr} is within the range of the harzburgite X_{Cr}. A higher X_{Cr} is to be expected if the dunite was a product of higher degrees of partial melting. On the other hand, an increasing degree of partial melting from the harzburgite with low X_{Cr} is possible on the basis of their geochemical characteristics (Fig. 9A). The pyroxenite exhibits a very limited range of X_{Cr} (0.51–0.54) along with a wide range of TiO_2 (wt%) concentrations (0.28 to 0.54). Although fractional crystallization is inferred to have occurred among the layered ultramafic cumulate rocks on the basis of mineral chemistry data, the mineral composition also suggests either the existence of several melts or mantle-melt interaction could have occurred during the evolution of these rocks (e.g., Zhou et al., 2001). A combination of these varying processes is also possible.

The nominal blocking temperature using Wells's (1977) two-pyroxene geothermometer for the residual and cumulate rocks yielded a limited range of 900–920°C. The olivine-spinel geothermometer for the ultramafic rocks gave a range of 650–900°C. Because plagioclase is present in the rocks, the pressure during the formation of these rocks must have been < 5 kbar.

It is evident that the harzburgite underwent partial melting, with the resulting melts responsible for the formation of some of the associated cumulate and volcanic-hypabyssal rocks. Fractional crystallization, mantle-melt interaction, primitive melt replenishment with accompanying magma mixing, and melt impregnation as suggested by the vermicular plagioclase are some of the processes involved in the evolution of this crust-mantle sequence. As recognized in other crust-mantle sequences, this would be possible in an open-system magma chamber that sourced its magmas from peridotite that had undergone varying degrees of partial melting (e.g., Yumul, 1989; Kogiso and Hirschmann, 2001).

Geodynamic Implications

The eastern portion of the Philippine archipelago is dotted by crust-mantle sequences that possess island-arc to MOR geochemical affinities. From north to south, northeastern and southeastern Luzon host ophiolite basement complexes showing MOR and suprasubduction-zone affinities (Geary and Kay, 1989; Billedo et al., 1996; David et al., 1996; Tamayo et al., 1996). Farther south in Samar and Dinagat islands, the ophiolite fragments in these islands host economic deposits of chromitite and platinum-group minerals. The observed mineralization is associated with the suprasubduction origin of these ophiolites (Yumul et al., 1997). Leyte island also hosts an ophiolite and our preliminary data suggest that it is supra-subduction zone related (e.g. Tamayo, 2001). Ophiolites also outcrop along eastern Mindanao, although their origin is still poorly constrained. Most workers invoke a proto-Philippine Sea plate for the origin of these ophiolites (Yumul et al., 2003; Tamayo et al., 2004).

The Rapu-Rapu ophiolite complex, which exhibits geochemical signatures within the range defined by the different eastern Philippine ophiolites, is a sample of Cretaceous oceanic lithosphere that could have been part of the proto-Philippine Sea plate. Variations in the geochemistry of the different ophiolites along the eastern Philippines may indicate either the presence of several small marginal basins within a larger proto-Philippine Sea plate or a single marginal basin with varying geochemical characteristics. There are present-day examples of both these possibilities. The present-day Philippine Sea plate is comprised of the West Philippine Basin, the Shikoku Basin, the Parece-Vela Basin, and the Marianas Trough. Several marginal basins (e.g., the West Philippine Basin, Okinawa Trough) exhibit varying geochemical crustal affiliations.

The Philippine archipelago, being at the junction of at least two plates—the Sundaland and Philippine Sea plates—had undergone many stages of deformation and tectonic upheavals. The Philippine mobile belt, bounded by large-scale faults, was rotated and translated northwestward from the Indo-Australian margin during the Eocene. Future studies should constrain the age and manner of emplacement of the different segments of oceanic lithosphere on the archipelago as well as provide information on how some portions of the proto-Philippine Sea plate were consumed, and why some were accreted, emplaced, and exposed.

Conclusions

The geological and geochemical study we have conducted on the Rapu-Rapu ophiolite complex led us to the following conclusions.

1. Rapu-Rapu Island can be divided into two blocks—Malobago and Pitogo. The Malobago block is characterized by a metamorphic rock sequence of chlorite quartz schist, quartzofeldspathic mica schist, and quartz sericite schist. Amphibolite is also present. Volcanogenic massive sulfides occur in this block. The Pitogo block exposes a complete ophiolite sequence, the Rapu-Rapu ophiolite complex.

2. The Rapu-Rapu ophiolite complex was formed in an intermediate to fast=-spreading ridge.

3. Petrographic and geochemical data suggest limited involvement of subduction during formation of this complex. The ophiolite displays geochemical

signatures chiefly similar to modern-day marginal basins.

4. Fractional crystallization, mantle-melt interaction, and limited melt replenishment–magma mixing were some of the processes that controlled the igneous evolution in the Rapu-Rapu ophiolite complex. The relict magma chamber operated as an open system.

5. The Rapu-Rapu ophiolite complex forms part of the eastern Philippine ophiolite belt characterized by crust-mantle sequences of varying geochemical affiliations. The Rapu-Rapu crust-mantle sequence originated from the proto-Philippine Sea plate.

Acknowledgments

Partial financial and logistic support came from the University of the Philippines–National Institute of Geological Sciences (UP-NIGS). Field support was provided by TVI Philippines, Inc. A Lepanto Consolidated Co. Inc. Professorial Chair to GPY is acknowledged with thanks. Analysis performed at the Geological Institute, University of Tokyo was made possible by a Japan Society for the Promotion of Scientific research fellowship to GPY. K. Ozawa, H. Nagahara-Takahashi, and H. Yoshida are thanked for the discussions. We would like to acknowledge our UP-NIGS Geology 215 students and other members of the Rushurgent Working Group who helped us map the island. Ross Sherlock is thanked for all the help extended during our survey in Rapu-Rapu Island. Discussions with him allowed a better understanding on how the metamorphic rock and mineralization in the island had evolved. J. V. de Jesus, F. A. Jimenez, Jr., F. O. Olaguera, and T. Tam III helped in drafting figures. The invitation to participate in the IGCP 434 project by Professor H. Hirano is appreciated. This paper was presented at the Tibet IGCP 434 meeting that was organized by Xiaoqiao Wan. Comments on a first draft of the paper by D. J. Batten and H. C. Jenkyns are appreciated. This is NIGS Contribution No. 2005-01.

REFERENCES

Barnes, S. J., and Roeder, P. L., 2001, The range of spinel compositions in terrestrial mafic and ultramafic rocks: Journal of Petrology, v. 42, p. 2279–2302.

Barrett, T. J., and MacLean, W. H., 1999, Volcanic sequences, lithogeochemistry, and hydrothermal alteration in some bimodal volcanic-associated massive sulfide systems: Reviews in Economic Geology, v. 8, p. 101–131.

Beard, J. S., 1986, Characteristic mineralogy of arc-related cumulate gabbros: Implications for the tectonic setting of gabbroic plutons and for andesite genesis: Geology, v. 14, p. 848–851.

Benoit, M., Ceuleneer, G., and Polve, M., 1999, The remelting of hydrothermally altered peridotite at mid-ocean ridges by intruding mantle diapirs: Nature, v. 402, p. 514–518.

Billedo, E., Stephan, J. F., Delteil, J., Bellon, H., Sajona, F. G., and Feraud, G., 1996, The pre-Tertiary ophiolitic complex of Northeastern Luzon and the Polillo Group of Islands, Philippines, *in* Yumul, G. P., Jr., and Manjoorsa, M. V., eds., special issue on the Ophiolites and Ophiolitic Complexes of the Philippines: Journal of the Geological Society of the Philippines, v. 51, p. 95–114.

Bloomer, S. H., Taylor, B., MacLeod, C. J., Stern, R. J., Fryer, P., Hawkins, J. W., and Johnson, L., 1995, Early arc volcanism and the ophiolite problem: A perspective from drilling in the western Pacific, *in* Taylor, B., and Natland, J., eds., Active margins and marginal basins of the western Pacific: American Geophysical Union Geophysical Monograph, v. 88, p. 1–30.

Boynton, W. V., 1984, Geochemistry of the rare earth elements: Meteorite studies, *in* Henderson, P., ed., Rare earth element geochemistry: Amsterdam, The Netherlands, Elsevier, p. 63–114.

Brunelli, D., Cipriani, A., Ottolini, L., Peyve, A., and Bonatti, E., 2003, Mantle peridotites from the Bouvet Triple Junction Region, South Atlantic: Terra Nova, v. 15, p. 194–203.

Bureau of Mines and Geosciences, 1982, Geology and mineral resources of the Philippines, v. 1. Manila, Philippines, Philippine Ministry of Natural Resources, 406 p.

Coish, R. A., and Gardner, P., 2004, Suprasubduction-zone peridotite in the northern USA Appalachians: Evidence from mineral composition: Mineralogical Magazine, v. 68, p. 699–708.

David, S. D. Jr., Stephan, J. F., Delteil, J., Bellon, H., and Sajona, F. G., 1996, Geology, geochemistry, geochronology and structures of the ophiolites in southeastern Luzon, Philippines, *in* Yumul, G. P., Jr., and Manjoorsa, M. V., eds., special issue on the Ophiolites and Ophiolitic Complexes of the Philippines: Journal of the Geological Society of the Philippines, v. 51, p. 115–129.

David, S. D. Jr., Stephan, J. F., Delteil, J., Muller, C., Butterlin, J., Bellon, H., and Billedo, E., 1997, Geology and tectonic history of southeastern Luzon, Philippines: Journal of Asian Earth Sciences, v. 15, p. 435–452.

Deschamps, A., Monie, P., Lallemand, S., Hsu, S. K., and Yeh, K. Y., 2000, Evidence for Early Cretaceous oceanic crust trapped in the Philippine Sea plate: Earth and Planetary Science Letters, v. 179, p. 503–516.

Dick, H. J. B., 1977, Partial melting in the Josephine peridotite. I. The effect on mineral composition and its consequence for geobarometry and geothermometry: American Journal of Science, v. 227, p. 801–832.

Dick, H. J. B., and Bullen, T., 1984, Chromian spinel as a petrogenetic indicator in abyssal and alpine-type peridotites and spatially associated lavas: Contributions to Mineralogy and Petrology, v. 86, p. 54–76.

Dilek, Y., Moores, E. M., and Furnes, H., 1998, Structure of modern oceanic crust and ophiolites and implications for faulting and magmatism at oceanic spreading centers, *in* Buck, W. R. et al., eds., Faulting and magmatism at mid-oceanic ridges: American Geophysical Union, Geophysical Monograph, v. 106, p. 219–265.

Falloon, C. A., Gree, D. H., Jacques, A. L., and Hawkins, J. W., 1999, Refractory magmas in back-arc basin settings: Experimental constraints on the petrogenesis of a Lau basin example: Journal of Petrology, v. 40, p. 255–277.

Faure, M., Marchadier, Y., and Rangin, C., 1989, Pre-Eocene synmetamorphic structure in the Mindoro-Romblon-Palawan area, West Philippines and implications for the history of Southeast Asia: Tectonics, v. 8, p. 963–979.

Geary, E. E., Harrison, T. M., and Heizler, M., 1988, Diverse ages and origins of basement complexes, Luzon, Philippines: Geology, v. 16, p. 341–344.

Geary, E. E., and Kay, R. W., 1989, Identification of an early Cretaceous ophiolite in the Camarines Norte-Calaguas Island basement complexes, eastern Luzon, Philippines: Tectonophysics, v. 168, p. 109–126.

Gribble, R. F., Stern, R. J., Newman, S., Bloomer, S. H., and O'Hearn, T., 1998, Chemical and isotopic composition of lavas from the northern Mariana trough: Implications for magma genesis in back-arc basins: Journal of Petrology, v. 39, p. 125–154.

Hall, R., 1996, Reconstructing Cenozoic SE Asia, *in* Hall, R., and Blundell, D., eds., Tectonic evolution of Southeast Asia: Geological Society of London, Special Publication, v. 106, p. 29–46.

Hall, R., 2002, Cenozoic geological and plate tectonic evolution of SE Asia and the SW Pacific: Computer-based reconstructions, models, and animations: Journal of Asian Earth Sciences, v. 20, p. 353–431.

Hawkins, J. W., 1995, Evolution of the Lau basin—insights from ODP Leg 135, *in* Taylor, B., and Natland, J., eds., Active margins and marginal basins of the western Pacific: American Geophysical Union Geophysical Monograph, v. 88, p. 125–173.

Jaques, A. L., 1981, Petrology and petrogenesis of cumulate peridotites and gabbros from the Marum ophiolite complex, northern Papua New Guinea: Journal of Petrology, v. 22, p. 1–40.

Jaques, A. L., and Green, D. H., 1980, Anhydrous melting of peridotite at 0–15 kbar pressure and the genesis of tholeiitic basalts: Contributions to Mineralogy and Petrology, v. 73, p. 287–310.

Jenner, G. J., Longerich, H. P., Jackson, S. E., and Fryer, B. J., 1990, ICP-MS: A powerful tool for high precision trace-element analysis in earth sciences: Evidence from analysis of selected USGS reference samples: Chemical Geology, v. 83, p. 133–148.

Kamenestky, V. S., Crawford, A. J., and Meffre, S., 2001, Factors controlling chemistry of magmatic spinel: An empirical study of associated olivine, Cr-spinel, and melt inclusions from primitive rocks: Journal of Petrology, v. 42, p. 655–671.

Koga, K. T., Kelemen, P. B., and Shimizu, N., 2001, Petrogenesis of the crust-mantle transition zone and the origin of lower crustal wehrlite in the Oman ophiolite: Geochemistry, Geophysics, and Geosystems 2 (paper number 2000GC000132 [words, figures, tables], July 2, 2001).

Kogiso, T., and Hirschmann, M. M., 2001, Experimental study of clinopyroxenite partial melting and the origin of ultra-calcic melt inclusions: Contributions to Mineralogy and Petrology, v. 142, p. 347–360.

Nakamura, Y., and Kushiro, I., 1970, Compositional relations of coexisting orthopyroxene, pigeonite, and augite in a tholeiitic andesite from Hakone Volcano: Contributions to Mineralogy and Petrology, v. 26, p. 265–275.

Parkinson, I. J., and Pearce, J. A., 1998, Peridotites from the Izu-Bonin-Marianas Forearc (ODP Leg 125): Evidence for mantle melting and melt-mantle interaction in a supra-subduction zone setting: Journal of Petrology, v. 39, p. 1577–1618.

Pearce, J. A., Lippard, S. J., and Robert, S., 1984, Characteristics and significance of supra-subduction zone ophiolites, *in* Kokelaar, B. P., and Howell, M. F., eds., Marginal basin geology: Geological Society of London, Special Publications, v. 16, p. 77–94.

Pfander, J. A., Jochum, K. P., Kozakov, I., Kroner, A., and Todt, W., 2002, Coupled evolution of back-arc and island arc–like mafic crust in the late Neoproterozoic Agardagh Tes–Chem ophiolite, Central Asia: Evidence from trace element and Sr-Nd-Pb isotope data: Contributions to Mineralogy and Petrology, v. 143, p. 154–174.

Pubellier, M., Monnier, C., and Ali, J., 2003, Cenozoic plate interaction of the Australia and Philippine Sea plates: "Hit and run" tectonics: Tectonophysics, v. 363, p. 181–199.

Querubin, C. L., and Yumul, G. P., Jr., 2001, The Malusok volcanogenic massive sulfide deposits, Siocon, Zamboanga del Norte, Mindanao, Philippines: Resource Geology, v. 51, p. 135–143.

Sato, H., 1977, Nickel content of basaltic magmas: Identification of primary magmas and a measure of the degree of olivine fractionation: Lithos, v. 10, p. 113–120.

Saunders, A. D., and Tarney, J., 1984, Geochemical characteristics of basaltic volcanism within back-arc basins, *in* Kokelaar, B. P., and Howells, M. F., eds., Marginal basin geology: Volcanic and associated sedimentary and tectonic processes in modern and ancient marginal basins: Geological Society Special Publication, v. 16, p. 59–76.

Sherlock, R. L., Barrett, T. J., and Lewis, P. D., 2003, Geological setting of the Rapu-Rapu gold-rich volcanogenic massive sulfide deposits, Albay Province, Philippines: Mineralium Deposita, v. 38, p. 813–830.

Shervais, J., 2001, Birth, death, and resurrection: The life cycle of suprasubduction zone ophiolites: Geochemistry, Geophysics, and Geosystems 2 (paper number 2000GC000080 [words, figures, tables. July 2, 2001).

Sun, S. S., and McDonough, W. F., 1989, Chemical and isotopic systematics of oceanic basalts: Implications for mantle composition and process, *in* Saunders, A. D., and Norry, M. J., eds., Magmatism in the ocean basins: Geological Society of London, Special Publication, v. 42, p. 313–345.

Takahashi, N., 2001, Origin of plagioclase lherzolite from the Nikanbetsu Peridotite Complex, Hokkaido, northern Japan: Implications for incipient melt migration and segregation in the partially molten upper mantle: Journal of Petrology, v. 42, p. 39–54.

Tamayo, R. A., Jr., 2001, Caractérisation pétrologique et géochimique origines et evolutions géodynamiques des ophiolites des Philippines: Unpubl. Ph.D. thesis, University of Bretagne Occidentale, France, 284 p.

Tamayo, R. A., Jr., Maury, R. C., Yumul, G. P., Jr., Polve, M., Cotten, J., Dimalanta, C. B., and Olaguera, F. O., 2004, Subduction-related magmatic imprint of most Philippine ophiolites: Implications on the early geodynamic evolution of the Philippine archipelago: Bulletin of the Geological Society of France, v. 175, p. 443–460.

Tamayo, R. A., Jr., Yumul, G. P. Jr., and Jumawan, F. T., 1996, Geology and geochemistry of the mafic rock series of the Camarines Norte Ophiolite Complex, *in* Yumul, G. P., Jr., and Manjoorsa, M. V., eds., Special issue on the Ophiolites and Ophiolitic Complexes of the Philippines: Journal of the Geological Society of the Philippines, v. 51, p. 131–152.

Tamayo, R. A. Jr., Yumul, G. P., Jr., Maury, R. C., Polve, M., Cotten, J., Bohn, M., and Olaguera, F. O., 2001, Preliminary geochemical and mineral data from the Isabela-Aurora ophiolite, northeastern Luzon, Philippines: InterRidge News, v. 10, p. 50–53.

Wang, Z., Sun, S., Li, J., and Hou, Q., 2002, Petrogenesis of tholeiite associations in Kudi ophiolite (western Kunlun Mountains, northwestern China: Implications for the evolution of back-arc basins: Contributions to Mineralogy and Petrology, v. 143, p. 471–483.

Wells, P. R. A., 1977, Pyroxene thermometry in simple and complex systems: Contributions to Mineralogy and Petrology, v. 62, p. 129–139.

Wolfe, J. A., 1981, Philippine geochronology: Journal of the Geological Society of the Philippines, v. 35, p. 1–30.

Xu, J-F., Castillo, P. R., Chen, F.-R., Niu, H.-C., Yu, X.-Y., and Zhen, Z.-P., 2003, Geochemistry of late Paleozoic mafic igneous rocks from the Kuerti area, Xinjiang, northwest China: Implications for back-arc mantle evolution: Chemical Geology, v. 193, p. 137–154.

Yoshida, H., and Takahashi, N., 1997, Chemical behavior of major and trace elements in the Horoman mantle diapir, Hidaka belt, Hokkaido, Japan: Journal of Mineralogy and Petrology, v. 92, p. 391–409.

Yumul, G. P., Jr., 1989, Petrological characterization of the residual-cumulate sequence of the Zambales Ophiolite Complex, Luzon, Philippines: Ofioliti, v. 14, p. 253–291.

Yumul, G. P., Jr., 1992, Ophiolite-hosted chromite deposits as tectonic setting and melting degree indicators: Examples from the Zambales ophiolite complex, Luzon, Philippines: Mining Geology, v. 42, p. 5–17.

Yumul, G. P., Jr., 1993, Angat ophiolitic complex, Luzon, Philippines: A Cretaceous dismembered marginal basin ophiolitic complex: Journal of Southeast Asian Earth Sciences, v. 8, p. 529–537.

Yumul, G. P., Jr., 2003, The Cretaceous Southeast Bohol ophiolite complex, central Philippines: Evidence for formation in a fast spreading center: Journal of Asian Earth Sciences, v. 21, p. 957–965.

Yumul, G. P., Jr., Balce, G. R., Dimalanta, C. B., and Datuin, R. T., 1997, Distribution, geochemistry, and mineralization potentials of Philippine ophiolite and ophiolitic sequences: Ofioliti, v. 22, 47–56.

Yumul, G. P., Jr., De Jesus, J. V., and Jimenez, F. A., Jr., 2001, Collision boundaries along the western Philippine archipelago: Gondwana Research, v. 4, p. 837–838.

Yumul, G. P. Jr., Dimalanta, C. B., Tamayo, R. A., Jr., and Maury, R. C., 2003, Collision, subduction, and accretion events in the Philippines: A synthesis: The Island Arc, v. 12, p. 77–91.

Yumul, G. P., Dimalanta, C. B., Tamayo, R. A., Jr., Maury, R. C., Bellon, H. B., Polve, M., Maglambayan, V. B., Querubin, C. L., and Cotten, J., 2004, Geology of the Zamboanga Peninsula, Mindanao, Philippines: An enigmatic South China continental fragment?, *in* Malpas, J., Fletcher, C. J. N., Ali, J. R., and Aitchison, J. C., eds., Aspects of the tectonic evolution of China: Geological Society of London Special Publication, v. 226, p. 289–312.

Zhou, M.-F., Robinson, P. T., Malpas, J., Aitchison, J., Sun, M., Bai, W.-J., Hu, X.-F., and Yang, J. S., 2001, Melt/mantle interaction and melt evolution in the Sartohay high-Al chromite deposits of the Dalabute ophiolite (NW China): Journal of Asian Earth Sciences, v. 19, p. 517–534.